The 3D structure of the Ring Nebula

W. Steffen[1], J.A. López[1], N. Koning[2], S. Kwok[2,3], H. Riesgo[1], M.G. Richer[1] and C. Morisset[4]

1. Instituto de Astronomía, Universidad Nacional Autónoma de México, Ensenada, Baja California, Mexico, wsteffen@astrosen.unam.mx
2. Department of Physics and Astronomy, University of Calgary, Calgary, Canada
3. Department of Physics, University of Hong Kong, Hong Kong
4. Instituto de Astronomía, Universidad Nacional Autónoma de México, Mexico City, Mexico

Summary. The Ring nebula (M57) is one of the closest and best observed planetary nebulae. Still, its structure remains controversial. Based on detailed spectroscopic observations of the kinematics we present a solution generated with SHAPE to the 3D structure of the [NII] emission. Assuming that the inner halo is the result from enhanced illumination from the central star through the holes of the inner nebula, we solve the geometry of the nebula.

Key words: M57, Ring Nebula, kinematics, 3D Modeling, Software

1 Introduction

The Ring Nebula (M 57, NGC 6720) is one of the closest and best observed planetary nebulae, yet its 3D structure has remained controversial (see Fig. 1). Although its projected appearance is relatively simple, studies of its emissivity distribution (e.g. Curtis 1918, Lousie 1974, Masson 1990) show that this does not correspond to an ellipsoid with a smooth surface brightness distribution. The orientation of the main axis of the nebula nearly coincides with the line of sight which further complicates the interpretation of its volume geometry. Previous kinematic studies have yielded inconsistent results. Bryce, Balick & Meaburn (1994) interpret their long-slit line profiles as arising from an open bipolar structure seen pole-on, whereas Guerrero, Manchado & Chu (1997) using similar data describe the nebula as a closed prolate ellipsoid. Hiriart (2004) interprets the kinematics and distribution of H2 as distributed over a cylindrical surface with a slightly larger radius at the equator. In order to settle on the 3D structure of the Ring nebula we have obtained a thorough mapping of long-slit, spatially resolved echelle spectra over the nebula and the data have been combined with the code SHAPE (Steffen & López, 2006) to obtain a self-consistent interpretation of the projected image on the sky, the line profiles, and its 3D structure.

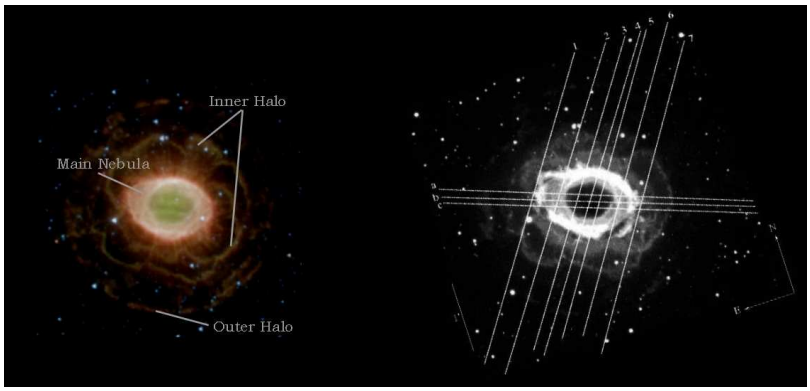

Fig. 1. Left: The Ring Nebula in the IR with definitions of its main regions. (Image: J. Hora (Harvard-Smithsonian CfA) (SSC/Caltech), JPL-Caltech, NASA). Right: Hα image with spectroscopic slit positions indicated.

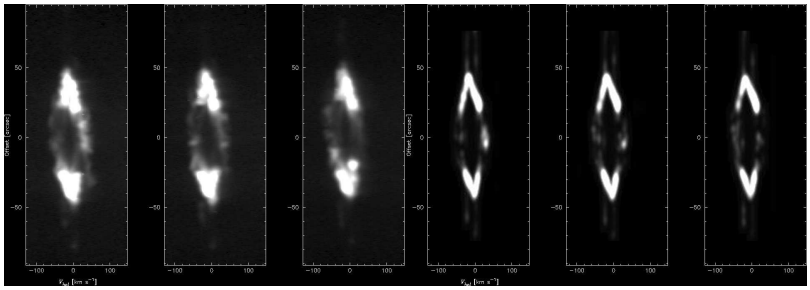

Fig. 2. Model long-slit pv-diagrams of M57 (3 right panels) produced with Shape are compared with the corresponding observations in [NII] (3 left panels). Slit positions are "a,b and c", from left to right.

2 The observations

The long-slit echelle spectra were obtained with MES-SPM (MEZCAL) spectrometer (Meaburn et al. 2004) on the 2.1 m telescope of the San Pedro Mártir Observatory (Mexico). Ten long-slit positions were obtained over the nebula, providing the best spatial coverage of this kind to date on the Ring Nebula (see Figure 1, right). The velocity resolution is 10 km s^{-1} and the seeing was 1 arcsec during the observations. Figures 2 and 3 show the P-V diagrams for the [N II] λ 6584 line corresponding to the 10 slit positions. The [NII] emission line is particularly well suited to analyze the global 3D structure of planetary nebulae, since it arises mainly in the transition regions between high and low ionization regions and is thus often confined to the outer 3D surface and in localized knots. Its intrinsic lower line width also allows better measurements of low velocity line splitting, as is the case in the outer regions of the Ring Nebula. For our modeling we did also take into account pv-diagrams from Guerrero, Manchado & Chu (1997).

3 Modeling with *Shape*

The morpho-kinematic modeling was done with *Shape* (Steffen & López, 2006). The emissivity distribution is constructed from a distribution of particles placed onto a 3D adaptive grid. This particle distribution is built using *3DStudioMax*[1]. The particles are distributed on a thick surface. The density distribution of the particles on the surface has been applied with standard mapping techniques, applying a grey-scale bitmap to the surface in spherical mapping coordinates. This bitmap was edited in an image editing program in such a way as to simultaneously reproduce the observed images and PV-diagrams. For the halos a procedural noise function was used for the particle density distribution.

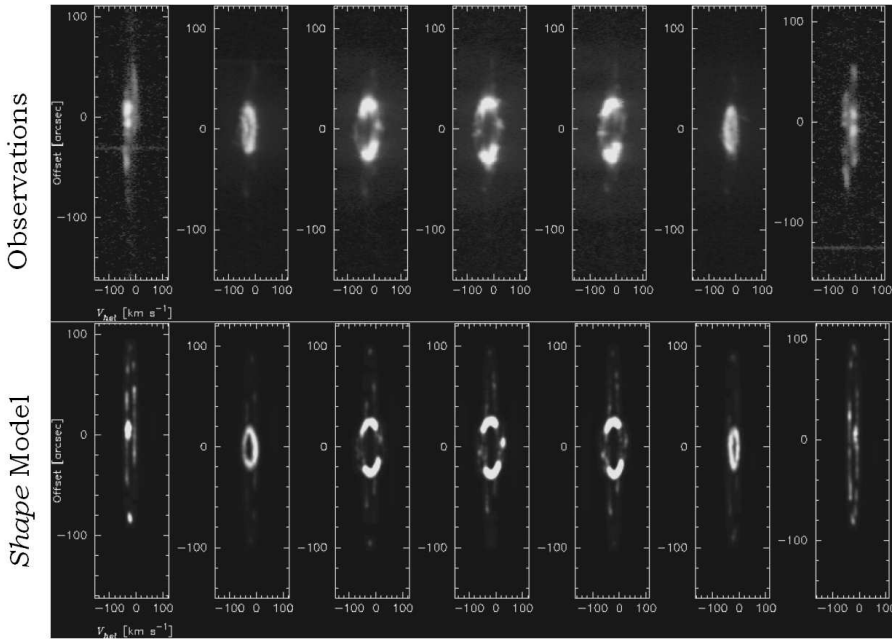

Fig. 3. Model long-slit pv-diagrams of M57 produced with Shape (bottom) are compared with the corresponding observations in [NII] (top). Slit positions are 1-7 (numbering from left to right).

4 Model assumption

In order to constrain the ambiguities inherent in the morpho-kinematic data, we make the following reasonable assumptions:
1. The circular outer halo is due to a clumpy thin spherical shell.

[1] *3DStudioMax* is a trademark of *Autodesk*

2. The inner halo is located at the same distance or within the outer halo (not only due to projection effects).
3. The inner halo is bright due to enhanced emission from the central star that escapes through the polar low density holes of the main nebula. Hence the outline of the inner halo is determined by the geometry of these holes into the halo volume.
4. The bright main (ring) nebula follows a hubble-law velocity field.
5. The halos follow the original AGB-wind velocity which is assumed constant at 15 km s^{-1}.

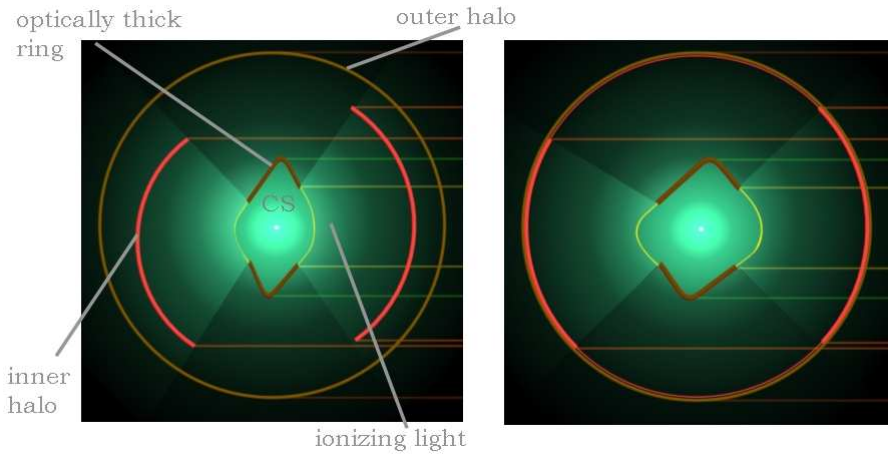

Fig. 4. Given the constraints from the observations (horizontal lines marking the projected positions of different regions), with our model only a small range of configurations is allowed for the structure of M57. The main nebula can be either slightly flattened (left) or have a line of sight that is limited by the observed dimensions of the axes of the main nebula. The position of the inner halo (red) varies only slightly in these cases.

5 Results

Figures 2 and 3 show the synthetic [N II] line profiles obtained from the Shape model along with the observations. The model reproduces most of the detailed features observed in the [NII] P-V diagrams with remarkable success. Our model for the main (Ring) nebula produces a deformed ellipsoid that is optically thick at the equator and thin at the poles, allowing ionizing radiation to escape and illuminate the inner halo. The model cannot precisely determine whether the ellipsoid is oblate or only slightly prolate. Both situations are depicted in Figure 4 where the orientation of the nebula has been rotated 90 degrees such the main axis of the Ring is now perpendicular to the line of sight. The left panel in Figure 4 shows the oblate case and the right panel the slightly prolate case where the opening angle of the emerging radiation and

outflows that outline the inner halo are the main difference among them. The *Shape* synthetic images are shown in Figure 5. Lines connecting the models in Figures 4 & 5 identify the different morphological components of the Ring nebula. The main symmetry axis of the Ring nebula is inclined by 10 degrees with respect to the line of sight.

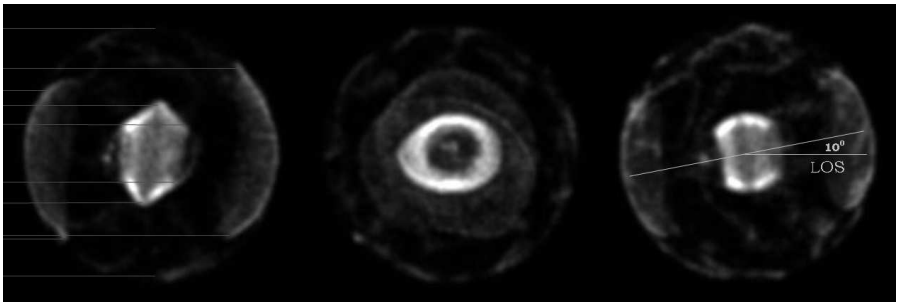

Fig. 5. Three different views of the rendered structure model of M57. The middle panel shows the view from Earth, while the others are views perpendicular to our line of sight. line correspond to the corresponding positions in Figure 4.

We have obtained a self-consistent morpho-kinematic model of the 3D structure of the Ring Nebula. The kinematic observations together with the assumption that the inner halo is a highly illuminated section of the AGB wind located within the outer halo fixes the geometry of the three main sections of the nebula (ring and the two halos) to an estimated margin of $10-20\%$. Details of this work will be published shortly (López et al., Steffen et al., in preparation).

Acknowledgement. This research has been supported by grants IN 108406-2, IN108506-2, 112103 from DGAPA, Universidad Nacional Autónoma de México, CONACYT grant 49447 and a grant from the Natural Sciences and Engineering Council of Canada awarded to Sun Kwok.

References

1. Bryce, M., Balick, B., Meaburn, J., 1994, MNRAS, 266, 721
2. Curtis, H.D., 1918, Pub. Lick. Obs., 13, 55
3. Guerrero, M.A., Manchado, A., Chu, Y.-H., 1997, 328-345
4. Hiriart, D., 2004, PASP, 116, 1135-1142
5. Louise, R., 1974, A&A, 30, 189
6. Meaburn, J., López, J.A., et al., 2003, RMxAA, 39, 185
7. Masson, C.R., 1990, ApJ, 348, 580-587
8. Steffen, W., López, J.A., 2004, ApJ, 612, 319-33
9. Steffen, W., López, J.A., 2006, RevMexAA, 42, 99-105